Development 133, 4613-4617 (2006) doi:10.1242/dev.02678

A dynamic fate map of the forebrain shows how vertebrate eyes form and explains two causes of cyclopia

Samantha J. England[1], Guy B. Blanchard[1], L. Mahadevan[2] and Richard J. Adams[1,*]

Mechanisms for shaping and folding sheets of cells during development are poorly understood. An example is the complex reorganisation of the forebrain neural plate during neurulation, which must fold a sheet into a tube while evaginating two eyes from a single contiguous domain within the neural plate. We, for the first time, track these cell rearrangements to show that forebrain morphogenesis differs significantly from prior hypotheses. We postulate a new model for forebrain neurulation and demonstrate how mutations affecting two signalling pathways can generate cyclopic phenotypes by disrupting normal cell movements or introducing new erroneous behaviours.

KEY WORDS: Zebrafish, Time-lapse microscopy, Neurulation, Cyclopia, Quantitative analyses

INTRODUCTION

Forebrain neurulation and common neural-tube defects associated with it, such as cyclopia (Gripp et al., 2000), are best studied dynamically so that normal movements and deviations from them can be directly measured. We have developed new methods to address this class of problem and in particular the early morphogenesis of the eye, using the transparent zebrafish as a model. Fate mapping studies in teleost fish, mouse and chick have shown that a significant anterior-posterior rearrangement of tissue takes place to relocate the hypothalamic anlagen (ventral diencephalon) from a position posterior to the eye field to one anterior and ventral to it (Woo and Fraser, 1995; Varga et al., 1999; Hirose et al., 2004; Inoue et al., 2000; Lawson, 1999; Cobos et al., 2001; Dale et al., 1999). This diencephalic rearrangement has been interpreted as splitting the early continuous eye field, with models favouring either a physical separation by a posterior to anterior movement of the future hypothalamus through the plane of the neural plate (Varga et al., 1999; Hirose et al., 2004), or a local induction of medial diencephalic tissue growth to bisect the eye field (Li et al., 1997). Reduced Nodal (Hatta et al., 1991; Hatta et al., 1994; Schier et al., 1996; Rebagliati et al., 1998; Sampath et al., 1998), Wnt11 (Heisenberg et al., 1996; Heisenberg and Nüsslein-Volhard, 1997; Heisenberg et al., 2000) or Sonic Hedgehog (Chiang et al., 1996) signalling results in cyclopia, a reduced interocular distance or eye fusion, it is presumed by altering forebrain patterning or morphogenesis. We have directly addressed this problem by producing time-lapse confocal movies of wild-type, *cyclops* (*cyc*) morphant and homozygous *silberblick*^{tx226} (*slb*) mutant zebrafish embryos. We labelled all cell nuclei with green fluorescent protein (GFP) to visualise and track their movements. In individual embryos, we tracked the paths of hundreds of cells contributing to the forebrain regions of eye, optic stalk, telencephalon, hypothalamus (ventral diencephalon) and dorsal diencephalon to generate high-resolution dynamic fate maps. Movements were followed from mid-gastrula (8 hours post fertilisation, hpf) in the anterior neural plate until the 18-somite stage (15 hpf) when forebrain domains are resolved by morphogenesis and cell fates could be assigned. This enables high-resolution visualisation and quantitative analysis of forebrain morphogenesis for the first time.

[1]Department of Physiology, Development and Neuroscience, University of Cambridge, Downing Street, Cambridge CB2 3DY, UK. [2]Division of Engineering and Applied Sciences, Harvard University, Pierce Hall, 29 Oxford Street, Cambridge, MA 02138, USA.

*Author for correspondence (e-mail: rja46@cam.ac.uk)

Accepted 4 October 2006

MATERIALS AND METHODS

Fish lines and genetics

Wild-type (AB) embryos were obtained from zebrafish (*Danio rerio*) lines raised at 28.5°C, maintained as described by Westerfield (Westerfield, 2000). Mutant embryos from homozygous *slb* carriers were a kind gift of Masazumi Tada (University College London, London, UK). Embryos were staged according to standard indicators (Kimmel et al., 1995).

RNA and morpholino injections

pCS2-nucGFP2 (a kind gift of Betsy Pownall, University of York, York, UK) was linearised by *Not*I, and capped mRNA transcripts were made using the MEGAscript SP6 in vitro transcription kit (Ambion). Embryos were injected at the one-cell stage with 80-100 pg of pCS2-nucGPF2 mRNA. *cyc* morphants were co-injected with 3 ng of *cyc* morpholino, as previously described (Karlen and Rebagliati, 2001).

Time-lapse imaging

Suitable embryos were dechorionated and mounted in 0.30% low gelling-temperature agarose (type VII, Sigma Aldrich) containing 0.017% tricaine (Sigma Aldrich) anaesthetic solution (Westerfield, 2000) in custom-built chambers (Concha and Adams, 1998) maintained at 28.5°C. Minimal volumes of embryo medium, containing 0.003% tricaine solution, were used to overlay embedded embryos.

Time-lapse imaging was performed using inverted laser scanning confocal microscopes: Zeiss LSM 510 and Leica Microsystems TSC-SP1-MP using long working-distance 20×/0.5 NA water immersion objectives. Image stacks of 50-60 sections of 2.8-3.2 μm spacing were recorded at 2-minute intervals for periods of 20 hours or more. Embryos were morphologically evaluated upon completion of imaging; any displaying abnormal development were excluded.

Cell tracking and data analysis

Manual and automated (G.B.B. and R.J.A., unpublished) cell tracking was performed using custom software written in Interactive Data Language (IDL, ITT Visual Information Solutions). Embryo shape was determined by detecting the embryos surface from its fluorescent signal. A blanket was fitted to this surface and the normals from this used to estimate the centroid of the embryo. Cell locations were expressed relative to this surface, giving a measure of radial depth within the embryo. Measures of the distances between forebrain regions were taken along the curved surface of the embryo, within a plane parallel to the anterior-posterior axis, passing through the centroid. These distances were also converted to relative angles by taking

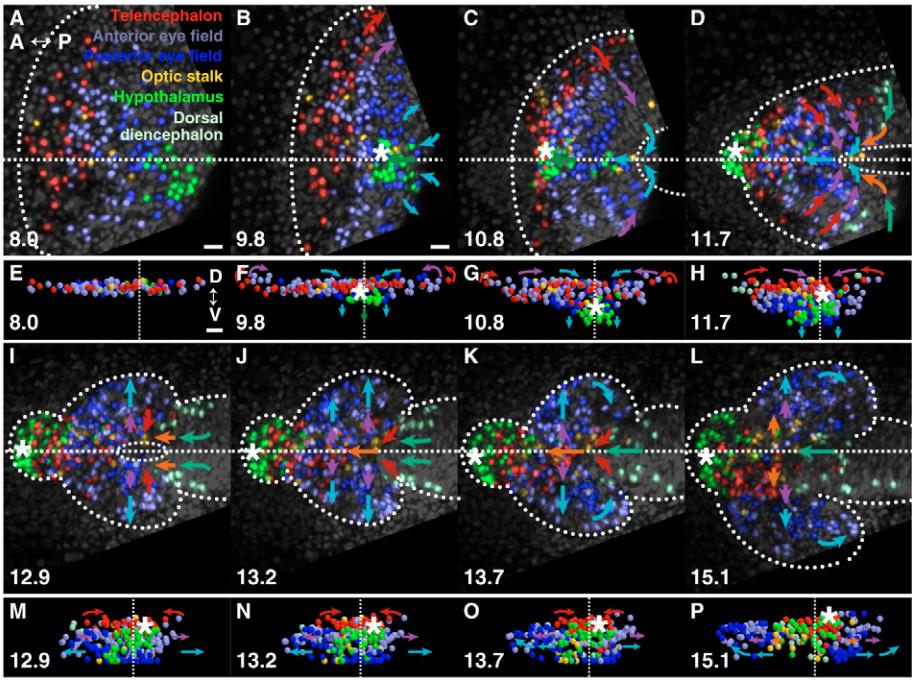

Fig. 1. Eye-field morphogenesis during forebrain neurulation.
(**A-D**,**I-L**) Projections of GFP-labelled nuclei (also see Movie 1 in the supplementary material). Dorsal projection, anterior is left. (**E-H**,**M-P**) 3D projections of tracked cells (also see Movies 2 and 3 in the supplementary material). Frontal projection, dorsal is up. (A,E) Forebrain regions prior to neurulation (midline, broken line). (B,F) Anterior neural plate contracts posteriorly towards the hypothalamic tip, where neural keel formation commences (asterisk). (C,G) Subducting hypothalamus moves anteriorly beneath the medial eye field. Convergence narrows the neural plate, which begins to fold lateral to medial, forming a neuropore (broken line). Posterior eye field moves anteriorly. (D,H) Hypothalamus emerges anterior and ventral, eye field remains contiguous across midline. (I,M) Eye evagination begins with cells moving into vesicles as posterior-lateral optic stalk and diencephalon converge and move anteriorwards. (J,N) Medial eye field continues to move into eye vesicles. (K,O) Lateral telencephalon meets at the midline to close the neuropore; anterior eye-field splitting is complete (arrows). Posterior optic stalk arrives beneath anterior stalk precursors. (L,P) Eye tissue now within eye vesicles. hpf, hours post fertilisation. Asterisks indicate anterior tip of neural keel formation (hypothalamus). Arrows indicate the direction of movement of the cells. Time (bottom left-hand corner) in hpf. Colours are indicated in A. A, anterior; P, posterior. Scale bars: 25 μm.

the angular displacement subtended by lines connecting the two locations to the centroid of the embryo. Angular measures were considered less prone to error when comparing measures in living and fixed embryos. Tissue deformation, expressed as contraction and expansion, was measured by calculating local velocity gradients (G.B.B., L.M. and R.J.A., unpublished). For each cell, gradients were calculated with respect to a fixed Cartesian system by looking at the movements of cells and their immediate neighbours. This velocity gradient was used to compute the principal direction and associated principal deformation rates by solving an eigenvalue problem. Cell velocities and positions were corrected for the effects of curvature of the embryo surface in these calculations.

RESULTS AND DISCUSSION

Tracking cells in wild-type animals confirms that hypothalamic precursors originate from a region medial and posterior to the eye field in the anterior neural plate (Fig. 1A) (Varga et al., 1999). The eye field begins as a broad bi-lobed domain bordered anteriorly by precursors of the telencephalon (Fig. 1A, Fig. 2A) and posteriorly by optic stalk. More peripherally there are dorsal diencephalon precursors (Fig. 1A,C) (S.J.E., G.B.B. and R.J.A., unpublished). Optic stalk precursors also originate more anteriorly among eye and telencephalic precursors (Fig. 1A).

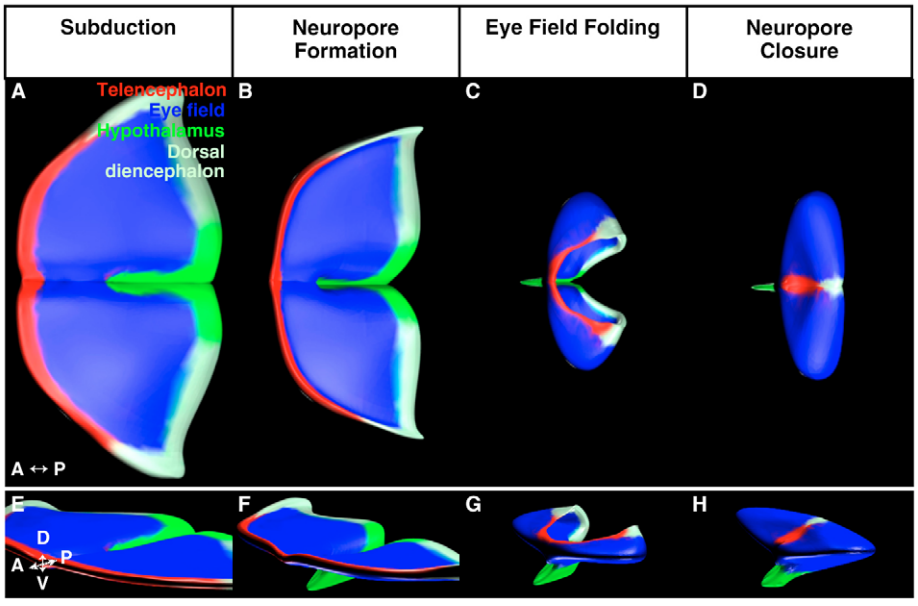

Fig. 2. Forebrain morphogenesis summary. (**A-H**) Frames from animations illustrating the principal forebrain-folding movements (also see Movies 4, 5 and 6 in the supplementary material). (A-D) Dorsal view, anterior is left. (E-H) Oblique view, anterior is bottom-left and dorsal is up. (A,E) The hypothalamus moves anteriorly beneath the medial eye field during subduction. The lateral edges of the neural plate begin folding towards the midline. (B,F) Lateral neural plate folds medial, forming a neuropore, below which eye-field tissue continues to fold. (C,G) Optic-vesicle formation begins as the diencephalon converges into the neural keel and moves anteriorwards. (D,H) The meeting of lateral telencephalon at the dorsal midline completes eye-field folding and closes the neuropore. Colours are indicated in A. A, anterior; P, posterior; D, dorsal; V, ventral.

Studies in the anterior trunk showed that neurulation in the zebrafish proceeds by folding of the neural plate about the midline to form a transient wedge of cells – the keel – in a mechanism analogous to primary neurulation in higher vertebrates (Papan and Campos-Ortega, 1994; Lowery and Sive, 2004). We show that neurulation within the forebrain is more complex, precluding neurulation through a simple keel or tube. Before neurulation, the most anterior neural plate begins posterior contraction towards a focus at the anterior tip of the hypothalamic anlagen (Fig. 1A, Fig. 3A,D,J,M). The onset of neurulation is detected and defined by a ventral movement of the hypothalamic anlagen, at the focus of contraction, to initiate formation of the anterior limit of the neural keel (Fig. 1B,F, Fig. 3A,D,G, and see Table S1 and Fig. S1 in the supplementary material). This keel subsequently subducts and extends beneath the eye field, without splitting it (Fig. 1C,G), and moves forward to emerge finally anterior to the telencephalic field (Fig. 1D,H, Fig. 3J,M). This posterior-to-anterior rearrangement maps to the dorso-ventral axis of the anterior neural tube (Fig. 3J,M). This movement in the epithelium results in a shear relative to the adjacent lateral tissue. Consequently, posterior eye cells are drawn deep and anteriorwards to begin eye folding (Fig. 1B-D,F-H, Fig. 3G). Coincidently, telencephalon and the anterior-lateral eye field fold towards the midline, which positions them above medial and posterior eye cells (Fig. 1B,F). This creates a neuropore within the dorsal seam of the neural tube near the site of subduction (Fig. 1C,D,G,H), which closes when the lateral edges meet at the midline (Fig. 1I-K,M-O). This folding initiates eye-vesicle evagination by forming an out-pocketing of tissue (Fig. 1I,M). Neurulation of the

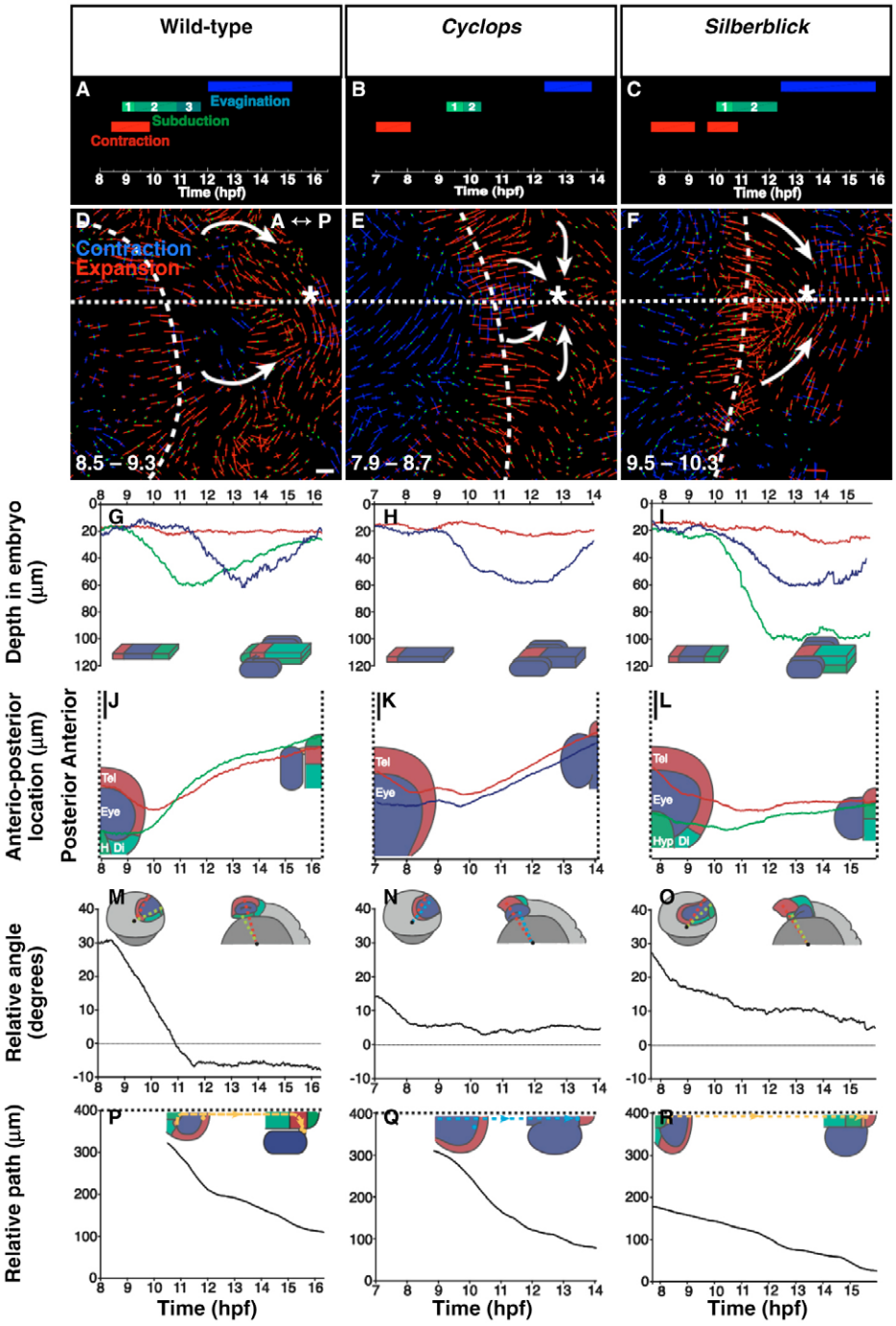

Fig. 3. Quantitative comparison of forebrain morphogenesis in wild type, *cyc* morphant and *slb*. (A,D,G,J,M,P) Wild type. (B,E,H,K,N,Q) *cyc* morphant. (C,F,J,L,O,R) *slb*. Dotted line, midline; dashed line, neural-plate border. (**A-C**) Timing of principal morphogenetic phases. Keel subduction is subdivided into: 1, moving deep; 2, moving forwards and deep; and 3, moving forwards. (**D-F**) Neural-plate contraction shown by a measure of tissue deformation. Dorsal view, anterior to left, as indicated. The orientations of deformation vectors show the principal directions and their length proportional to magnitude. Neural and non-neural ectoderm is distinct. In wild-type and *cyc* morphant embryos, keel initiation (asterisk) is coincident with the focal point of neural-plate contraction (arrows), but in *slb* these two behaviours are dissociated. (**G-I**) Depth within the embryo of medial tissue during keel formation. Hypothalamus undergoes subduction in wild type (G) and *slb* (I); the medial eye field subducts in *cyc* morphant (H). Telencephalon remains shallow in all cases. (**J-L**) Locations of the subducting tissues relative to the telencephalon, shown by location along the anterior-posterior axis. (**M-O**) The same data is plotted as angular positions measured around the great circle along the midline, relative to an arbitrary anterior reference point. (**P-R**) Rate of eye evagination was measured from the movement of posterior eye-field cells that remain connected to the neural tube, after evagination, relative to their anterior counterparts. These are future optic-stalk cells in wild type (P) and *slb* (R), and the residual band of retina in *cyc* morphant (Q). Positions were followed along the path of movement rather than the straight-line distance. Reduced anterior-posterior reorganisation in *slb* is evident. hpf, hours post fertilisation. (D,F) Time (bottom left-hand corner) in hpf. Colours for A-C,G-R are indicated in A; and for D-F in D. A, anterior; P, posterior. Scale bars: 25 μm.

dorsal forebrain far more closely resembles movements observed in higher vertebrates that involve folding within the neural plate rather than the use of a neural keel.

We find no evidence that the subducting hypothalamus bisects the eye field; in fact, these cells have predominantly converged medially during subduction and remain composed of intermixed precursors of left and right eyes (see Fig. S2A-H in the supplementary material). This is inconsistent with a simple physical displacement by the subducting hypothalamus (ventral diencephalon).

Evagination of the eyes proceeds by a combination of two principal movements. First, the dorsal diencephalon sweeps inwards and forwards, displacing eye and future optic-stalk tissue forwards and then out into the emerging optic vesicles (Fig. 1I-P, Fig. 3P). Second, anterior eye tissue at the midline displaces laterally from above into the eye vesicles as the telencephalon seals the neuropore to occupy the dorsal neural tube (Fig. 1J-K,N-O). This latter movement is predominantly coincident with the segregation of intermingled left and right eye cells into their respective eyes (see Fig. S2I-P in the supplementary material). This description of forebrain morphogenesis is summarised in Fig. 2.

Given this new model of neural-plate folding in the forebrain, we re-address how neurulation is disrupted in cyclopic mutants. In the *cyc* mutant, a loss of Ndr2 signalling causes abnormal patterning and morphogenesis of mesoderm and forebrain (Rebagliati et al., 1998; Sampath et al., 1998). After neurulation, a portion of the eye field remains medial as a band of eye tissue spanning the front of the brain between two partial eye cups (Macdonald et al., 1995; Fulwiler et al., 1997). The size and location of the presumptive eye field is normal in *cyclops* mutant and morphant embryos; however, hypothalamic tissue is not induced (Fig. 4D, see Fig. S1 in the supplementary material) (Varga et al., 1999). Tracking cells in *cyc* morphants, we show that the focus of neural-plate contraction (Fig. 3E), and the initiation of neural keel formation, locate within the eye field itself (Fig. 3H,N, Fig. 4E,J, see Table S1 and Fig. S1 in the supplementary material); this is far more anterior to the usual initiation in wild type, which corresponds to the anterior tip of the hypothalamus (Fig. 1B,F). This abnormal focus of contraction causes medial eye-field cells to be brought erroneously anterior and ventral within the neural tube (Fig. 3H,Q, Fig. 4F,L). Morphants additionally show reduced movements of the keel beneath the remaining eye and telencephalic fields: the keel never emerges anterior to them (Fig. 3K,N, Fig. 4F).

A consequence of attenuated subduction movements is that posterior eye tissue does not move forward within the neural plate (Fig. 3K, Fig. 4E,F,P-R). Convergence of telencephalic and anterior eye fields towards the midline is similar to the wild-type (Fig. 4E,F,J,L,P,T), but is not sufficient to resolve the eye-field cells within the keel into separate vesicles (Fig. 4Q,R,V,X). This shows that cyclopia in *cyclops* results in incorporation of eye tissue into an inappropriate location within the medial neural keel. We speculate that this precludes its resolution into the eye vesicles by any of the morphogenetic mechanisms observed so far in wild-type animals.

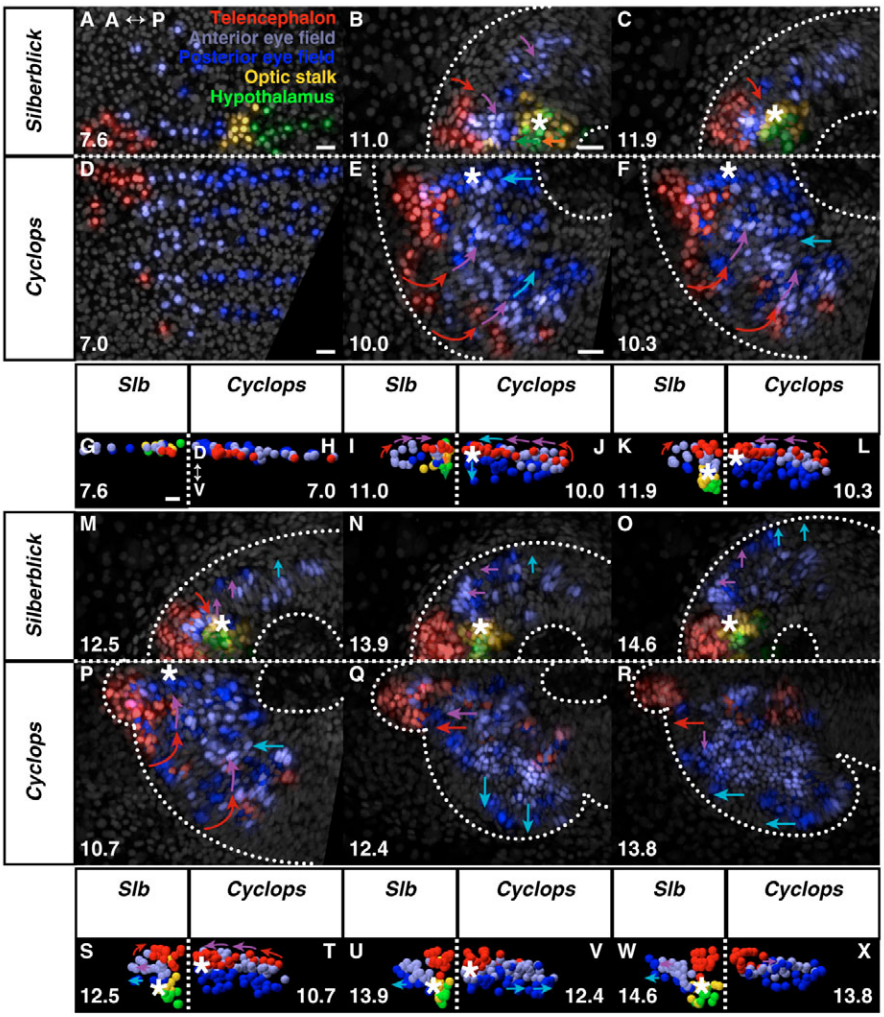

Fig. 4. Eye morphogenesis in *cyc* morphant and *slb*. (**A-F**,**M-R**) Dorsal projections, anterior to left; (**G-L**,**S-X**) frontal projections, dorsal up. *slb* (A,G) and *cyc* morphant (D,H) forebrain regions prior to neurulation. Anterior limit of keel formation, as with wild-type, begins with hypothalamus in *slb* (B) but is far anterior within the anterior eye field in *cyc* morphant (E). (C,F) Keel movement is attenuated in both *cyc* morphant and *slb*, relative to wild-type, never emerging anterior to the telencephalon. (I,K) Anterior tissue is displaced progressively deep in *slb*. (J,L) Medial eye field occupies the ventral midline in *cyc* morphant. (M-O) Retarded medial eye-field reorganisation and evagination in *slb*. (S,U,W) Deep keel persists in *slb*. (P,Q,T,V) Normal medial convergence of telencephalon and anterior eye field in *cyc* morphant. (R,X) Subducted eye field remains medial within keel after evagination. Square dotted line, midline. Asterisk, anterior tip of neural keel. Arrows indicate the direction of movement of the cells. Time (bottom left- or right-hand corner) in hpf. Colours are indicated in A. See Movies 7 (*slb*), 8 (*cyc* morphant), 9 and 10 in the supplementary material. A, anterior; P, posterior; D, dorsal; V, ventral; hpf, hours post fertilisation. Scale bars, 25 μm.

This represents a dissociation of the mechanisms of patterning and morphogenesis. These defects override potential mechanisms intrinsic to the eye field that usually result in eye separation, such as the motile capacity of eye-field cells (Rembold et al., 2006).

A second mutant, *slb*, which encodes Wnt11, shows incomplete eye-field separation (Heisenberg et al., 2000). This gene has been associated with reduced movements of convergence and extension, as well as aberrant migration of the mesoderm (Heisenberg and Nüsslein-Volhard, 1997; Hammerschmidt et al., 1996; Solnica-Krezel et al., 1996; Ulrich et al., 2003). Effects of Wnt11 on eye morphogenesis could be caused indirectly by disrupting mesodermal induction of neural patterning (Heisenberg and Nüsslein-Volhard, 1997; Marlow et al., 1998), or directly from Wnt11 expression in lateral neurectoderm, posterior to the presumptive forebrain (Heisenberg et al., 2000). We investigated eye-field morphogenesis in homozygous *slb* mutants. Forebrain territories, although patterned normally, are broadened and shortened (Fig. 3F, Fig. 4A, see Fig. S1 in the supplementary material) (Heisenberg et al., 1996), possibly because of defective convergence and extension. The focus of early contraction is less clearly resolved (Fig. 3F). However, the initiation of keel formation is at the anterior boundary of the hypothalamus, as observed in wild type (Fig. 3I,L,O, Fig. 4B,I, see Table S1 and Fig. S1 in the supplementary material). Anteriorward movement of the neural keel, however, is much reduced (Fig. 3L,O, Fig. 4C,K), as in *cyclops* (Fig. 3K,N), and the hypothalamus never emerges anterior to the telencephalon (Fig. 3L,O, Fig. 4C). Instead, the hypothalamus, optic stalk and posterior eye field are displaced progressively deeper within the keel (Fig. 3I, Fig. 4I,K). Along with a severely reduced convergence of the lateral neural plate, this slows folding of the lateral eye towards the midline (Fig. 4C). Compared with the extensive movement of lateral-posterior eye-field cells fated to optic stalk in wild type (Fig. 1D,H,I-P, Fig. 3P), much reduced convergent and forward movement of the *slb* eye field results in medial-posterior eye-field cells remaining medial (Fig. 3R, Fig. 4M-O,S,U,W). We postulate that this defect in movement is a major cause of the reduced resolution of bilateral eye fates in this class of mutant, constituting a second, temporally and spatially distinct, defect of forebrain morphogenesis. Analyses of these two mutants reveal two of the intrinsic steps that comprise the complex morphogenetic program of forebrain development.

We thank Bill Harris and members of the Adams group for discussion and critical reading of this manuscript; and many colleagues for providing reagents. We especially thank Masazumi Tada and Nina Buchan for providing *silberblick* mutant embryos. A Research Studentship from the BBSRC supported S.J.E. A MRC Senior Research Fellowship and Research Grant to R.J.A. supported this work.

Supplementary material

Supplementary material for this article is available at
http://dev.biologists.org/cgi/content/full/133/23/4613/DC1

References

Chiang, C., Litingtung, Y., Lee, E., Young, K. E., Corden, J. L., Westphal, H. and Beachy, P. A. (1996). Cyclopia and defective axial patterning in mice lacking Sonic hedgehog gene function. *Nature* **383**, 407-413.

Cobos, I., Shimamura, K., Rubenstein, J. L., Martinez, S. and Puelles, L. (2001). Fate map of the avian anterior forebrain at the four-somite stage, based on the analysis of quail-chick chimeras. *Dev. Biol.* **239**, 46-67.

Concha, M. L. and Adams, R. J. (1998). Oriented cell divisions and cellular morphogenesis in the zebrafish gastrula and neurula: a time-lapse analysis. *Development* **125**, 983-994.

Dale, K., Sattar, N., Heemskerk, J., Clarke, J. D., Placzek, M. and Dodd, J. (1999). Differential patterning of ventral midline cells by axial mesoderm is regulated by BMP7 and chordin. *Development* **126**, 397-408.

Fulwiler, C., Schmitt, E. A., Kim, J. M. and Dowling, J. E. (1997). Retinal patterning in the zebrafish mutant cyclops. *J. Comp. Neurol.* **381**, 449-460.

Gripp, K. W., Wotton, D., Edwards, M. C., Roessler, E., Ades, L., Meinecke, P., Richieri-Costa, A., Zackai, E. H., Massague, J., Muenke, M. et al. (2000). Mutations in TGIF cause holoprosencephaly and link NODAL signalling to human neural axis determination. *Nat. Genet.* **25**, 205-208.

Hammerschmidt, M., Pelegri, F., Mullins, M. C., Kane, D. A., Brand, M., van Eeden, F. J., Furutani-Seiki, M., Granato, M., Haffter, P., Heisenberg, C. P. et al. (1996). Mutations affecting morphogenesis during gastrulation and tail formation in the zebrafish, Danio rerio. *Development* **123**, 143-151.

Hatta, K., Kimmel, C. B., Ho, R. K. and Walker, C. (1991). The cyclops mutation blocks specification of the floor plate of the zebrafish central nervous system. *Nature* **350**, 339-341.

Hatta, K., Puschel, A. W. and Kimmel, C. B. (1994). Midline signaling in the primordium of the zebrafish anterior central nervous system. *Proc. Natl. Acad. Sci. USA* **91**, 2061-2065.

Heisenberg, C. P. and Nusslein-Volhard, C. (1997). The function of silberblick in the positioning of the eye anlage in the zebrafish embryo. *Dev. Biol.* **184**, 85-94.

Heisenberg, C. P., Brand, M., Jiang, Y. J., Warga, R. M., Beuchle, D., van Eeden, F. J., Furutani-Seiki, M., Granato, M., Haffter, P., Hammerschmidt, M. et al. (1996). Genes involved in forebrain development in the zebrafish, Danio rerio. *Development* **123**, 191-203.

Heisenberg, C. P., Tada, M., Rauch, G. J., Saude, L., Concha, M. L., Geisler, R., Stemple, D. L., Smith, J. C. and Wilson, S. W. (2000). Silberblick/Wnt11 mediates convergent extension movements during zebrafish gastrulation. *Nature* **405**, 76-81.

Hirose, Y., Varga, Z. M., Kondoh, H. and Furutani-Seiki, M. (2004). Single cell lineage and regionalization of cell populations during Medaka neurulation. *Development* **131**, 2553-2563.

Inoue, T., Nakamura, S. and Osumi, N. (2000). Fate mapping of the mouse prosencephalic neural plate. *Dev. Biol.* **219**, 373-383.

Karlen, S. and Rebagliati, M. (2001). A morpholino phenocopy of the cyclops mutation. *Genesis* **30**, 126-128.

Kimmel, C. B., Ballard, W. W., Kimmel, S. R., Ullmann, B. and Schilling, T. F. (1995). Stages of embryonic development of the zebrafish. *Dev. Dyn.* **203**, 253-310.

Lawson, K. A. (1999). Fate mapping the mouse embryo. *Int. J. Dev. Biol.* **43**, 773-775.

Li, H., Tierney, C., Wen, L., Wu, J. Y. and Rao, Y. (1997). A single morphogenetic field gives rise to two retina primordia under the influence of the prechordal plate. *Development* **124**, 603-615.

Lowery, L. A. and Sive, H. (2004). Strategies of vertebrate neurulation and a re-evaluation of teleost neural tube formation. *Mech. Dev.* **121**, 1189-1197.

Macdonald, R., Anukampa Barth, K., Xu, Q., Holder, N., Mikkola, I. and Wilson, S. W. (1995). Midline signaling is required for Pax gene regulation and patterning of the eyes. *Development* **121**, 3267-3278.

Marlow, F., Zwartkruis, F., Malicki, J., Neuhauss, S. C., Abbas, L., Weaver, M., Driever, W. and Solnica-Krezel, L. (1998). Functional interactions of genes mediating convergent extension, knypek and trilobite, during the partitioning of the eye primordium in zebrafish. *Dev. Biol.* **203**, 382-399.

Papan, C. and Campos-Ortega, J. A. (1994). On the formation of the neural keel and neural tube in the zebrafish *Danio (Brachydanio) rerio*. *Rouxs Arch. Dev. Biol.* **203**, 178-186.

Rebagliati, M. R., Toyama, R., Haffter, P. and Dawid, I. B. (1998). Cyclops encodes a nodal-related factor involved in midline signaling. *Proc. Natl. Acad. Sci. USA* **95**, 9932-9937.

Rembold, M., Loosli, F., Adams, R. J. and Wittbrodt, J. (2006). Individual cell migration serves as the driving force for optic vesicle evagination. *Science* **313**, 1130-1134.

Sampath, K., Rubinstein, A. L., Cheng, A. M., Liang, J. O., Fekany, K., Solnica-Krezel, L., Korzh, V., Halpern, M. E. and Wright, C. V. (1998). Induction of the zebrafish ventral brain and floorplate requires cyclops/nodal signaling. *Nature* **395**, 185-189.

Schier, A. F., Neuhauss, S. C., Harvey, M., Malicki, J., Solnica-Krezel, L., Stainier, D. Y., Zwartkruis, F., Abdelilah, S., Stemple, D. L., Rangini, Z. et al. (1996). Mutations affecting the development of the embryonic zebrafish brain. *Development* **123**, 165-178.

Solnica-Krezel, L., Stemple, D. L., Mountcastle-Shah, E., Rangini, Z., Neuhauss, S. C., Malicki, J., Schier, A. F., Stainier, D. Y., Zwartkruis, F., Abdelilah, S. et al. (1996). Mutations affecting cell fates and cellular rearrangements during gastrulation in zebrafish. *Development* **123**, 67-80.

Ulrich, F., Concha, M. L., Heid, P. J., Voss, E., Witzel, S., Roehl, H., Tada, M., Wilson, S. W., Adams, R. J., Soll, D. R. et al. (2003). Slb/Wnt11 controls hypoblast cell migration and morphogenesis at the onset of zebrafish gastrulation. *Development* **130**, 5375-5384.

Varga, Z. M., Wegner, J. and Westerfield, M. (1999). Anterior movement of ventral diencephalic precursors separates the primordial eye field in the neural plate and requires cyclops. *Development* **126**, 5533-5546.

Westerfield, M. (2000). *The Zebrafish Book. A Guide for the Laboratory Use of Zebrafish* (*Danio rerio*) (4th edn). Eugene: University of Oregon Press.

Woo, K. and Fraser, S. E. (1995). Order and coherence in the fate map of the zebrafish nervous system. *Development* **121**, 2595-2609.

Table S1. Locations of subducting tissues versus the anterior eye field in wild-type, *cyc* MO and *silberblick* embryos

Location	Relative angle (degrees)		
	Wild-type	*cyc* MO	*silberblick*
Medial anterior eye field versus initiation of keel formation*	30.29 (*n*=1)	5.56 (*n*=1)	19.52 (*n*=1)
Medial anterior eye field versus posterior eye field§	35.64±5.94 s.d. (*n*=3)	50.64±3.05 s.d. (*n*=3)	34.17±4.58 s.d. (*n*=6)

Cell fates were identified by live movie tracing (*) or by in situ analysis (§) (Fig. S1). Their locations, with respect to the medial anterior boundary of the eye field, were compared at 80% epiboly (8.4 hpf) by measuring the intervening angle subtended at the embryonic centroid. s.d., standard deviation.